

## **Ion Molecule Reactions in the HBr<sup>+</sup> + CH<sub>4</sub> System:**

### **A combined experimental and theoretical study**

Dominik Plamper <sup>a</sup>, Allen Vincent <sup>b</sup>, Kazuumi Fujioka <sup>b</sup>, Rui Sun <sup>\*b</sup> and Karl-Michael Weitzel <sup>\*a</sup>,

a. Philipps-Universität Marburg, Fachbereich Chemie, 35032 Marburg, Germany.

b. Department of Chemistry, University of Hawai'i at Manoa, Honolulu, Hawaii 96822, United States

\* Karl-Michael Weitzel: weitzel@chemie.uni-marburg.de

\* Rui Sun: ruisun@hawaii.edu

#### Table of content

1. Single-collision conditions.....	2
2. Mass spectrum for the reaction HBr <sup>+</sup> + CH <sub>4</sub> .....	3
3. Analysis of signals for HBr <sup>+</sup> + CH <sub>4</sub> .....	4
4. Rotational dependence of $\sigma_H$ .....	5
5. Rotational dependence of $\sigma_{CT}$ .....	6
6. Rotational dependence of $\sigma_{BT}$ .....	7
7. Supplementary Information – Potential energy surface of CH <sub>4</sub> + HBr <sup>+</sup> bimolecular reaction .....	8
8. Scattering angle distributions for collision energies (0.5 eV, 2.0 eV and 3.0 eV) respectively.....	13

## 1. Single-collision conditions

By adjusting the partial pressure of methane in a way that the mean free path is longer than the length of the reaction zone, single collision conditions are ensured.

$$\lambda_m = \frac{k_B \cdot T}{\sigma \cdot p_{RZ}} > l_{RZ} = 25 \text{ cm} \quad (\text{S1})$$

The mean free path is calculable by eq. (S1). In the experiment the collision energy  $E_{c.m.}$  was varied in the range from 0.25 eV up to 2.99 eV. This leads to cross sections, according to the Langevin theory, from 53.96 Å to 15.69 Å. Therefor the mean free path is in the range from 214.3 cm to 737.1 cm for a typically chosen pressure of  $3.5 \cdot 10^{-5}$  mbar. All measured cross sections lie below the predicted cross sections calculated by the Langevin model. For this reason the mean free path discussed above is an upper limit.

## 2. Mass spectrum for the reaction $\text{HBr}^+ + \text{CH}_4$

In Figure S1 a mass spectrum of the reaction system  $\text{HBr}^+ + \text{CH}_4$  in the range from 14 m/z to 86 m/z is shown.

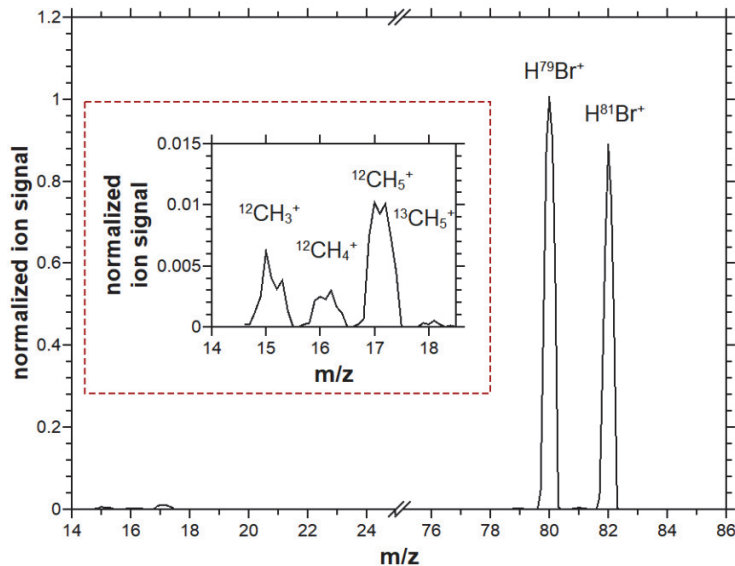


Figure S 1. Mass spectrum for the reaction system  $\text{HBr}^+ + \text{CH}_4$  from 14 m/z to 86 m/z.

The mass spectrum was acquired at a collision energy of 3 eV. The  $\text{HBr}^+$  ions were created via the R(1) transition and had 3.4 meV mean rotational energy ( $\langle E_{\text{rot}} \rangle$ ).

In Figure S2 the mass spectrum of the title reaction from m/z 76 to m/z 98 is shown.

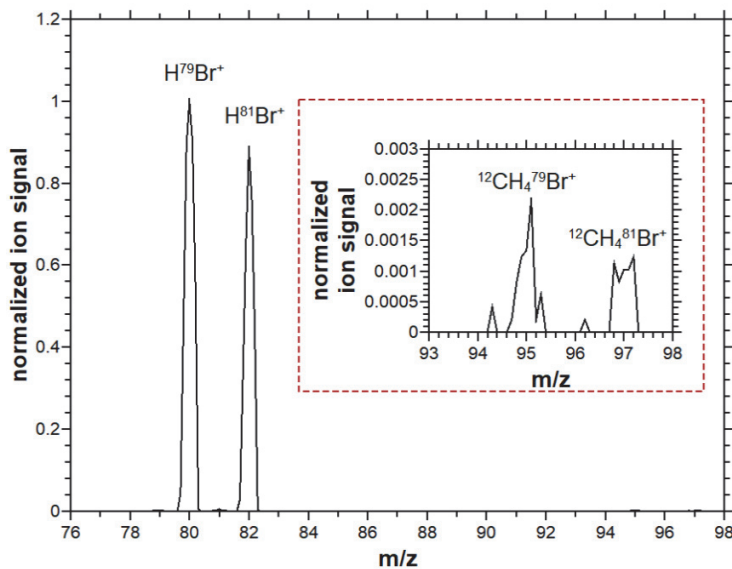


Figure S 2. Mass spectrum of the reaction system  $\text{HBr}^+ + \text{CH}_4$  from 76 m/z to 98 m/z.

### 3. Analysis of signals for HBr<sup>+</sup> + CH<sub>4</sub>

Both educt isotopes in the mass spectrum are the most intense one. The ion signal of the educt ion is calculated using eq. (S2). The product ions resulting from the <sup>13</sup>C isotope are considered to be negligible small in comparison to the <sup>12</sup>C isotope. Only the <sup>13</sup>CH<sub>5</sub><sup>+</sup> isotope is used for deriving cross sections because of the higher intensity of the PT reaction channel. With this approach the signal intensities for the product ions are calculated according to eq. (S3) to eq. (S5).

$$I_{\text{HBr}^+} = I_{80} + I_{82} \quad (\text{S2})$$

$$I_{\text{CH}_5^+} = I_{17} + I_{18} \quad (\text{S3})$$

$$I_{\text{CH}_4^+} = I_{16} \quad (\text{S4})$$

$$I_{\text{CH}_4\text{Br}^+} = I_{95} + I_{97} \quad (\text{S5})$$

These signal intensities are used to calculate the fractional abundance *f.a.*.

#### 4. Rotational dependence of $\sigma_{\text{HA}}$

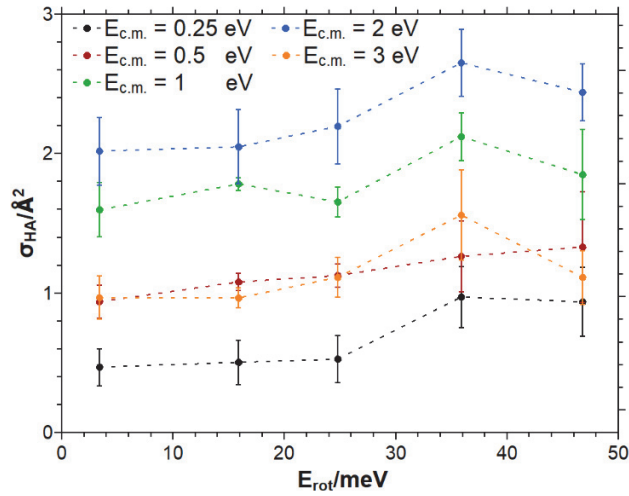


Figure S 3. Rotational energy dependence of the HA reaction for the investigated collision energies.

Figure S 3 shows the ion rotational energy dependence of the HA cross section. This rotational energy dependence is rather weak. From  $E_{\text{rot}}=24.8 \text{ meV}$  to  $E_{\text{rot}}=35.9 \text{ meV}$  the cross section slightly increases. Based on a canonical ensemble the mean rotational energy of methane amounts to  $1.5 k_B T$ . Given the rotational constant of methane  $B_{\text{neutral}} = 5.2412 \text{ cm}^{-1}$ <sup>53</sup> this mean rotational energy can be translated to a rotational velocity. Given furthermore a rotational constant of the HBr<sup>+</sup>  $B_{\text{ion}} = 7.91 \text{ cm}^{-1}$ <sup>54</sup> the neutral methane and the HBr<sup>+</sup> ion exhibit the same rotational velocity, when the rotational energy of the ion is  $E_{\text{rot}}(\text{HBr}^+) = 25.1 \text{ meV}$ . This turns out to be the energy, where the cross section for HA starts to rise. In previous work a minimum of the cross section was observed when the rotational velocity of the ion matched that of the neutral target.<sup>22</sup>.

## 5. Rotational dependence of $\sigma_{CT}$

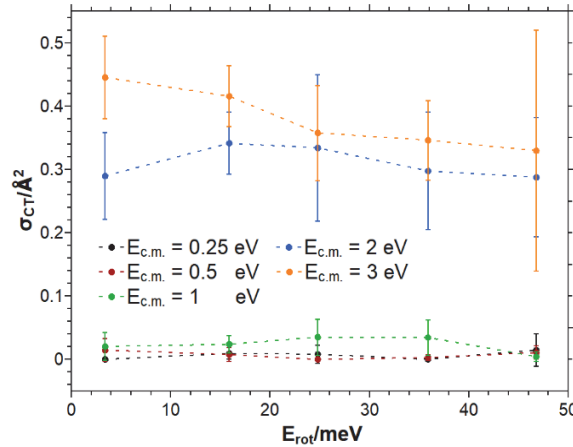


Figure S 4.  $\sigma_{CT}$  as a function of  $E_{\text{rot}}$  for different collision energies.

Figure S 4 shows  $\sigma_{CT}$  as a function of the rotational energy in the HBr<sup>+</sup> ion. Evidently, the cross section  $\sigma_{CT}$  is basically independent of the rotation within the error margins. The reaction threshold near 1 eV collision energy is clearly visible in this representation. The A parameter in Table 4 of the main text suggested a modest decrease with increasing  $E_{\text{rot}}$ , which is, however, not resolved in terms of the error bars. As the CT is independent of ion rotation this degree of freedom does not appear to contribute to the reaction coordinate.

## 6. Rotational dependence of $\sigma_{\text{BT}}$

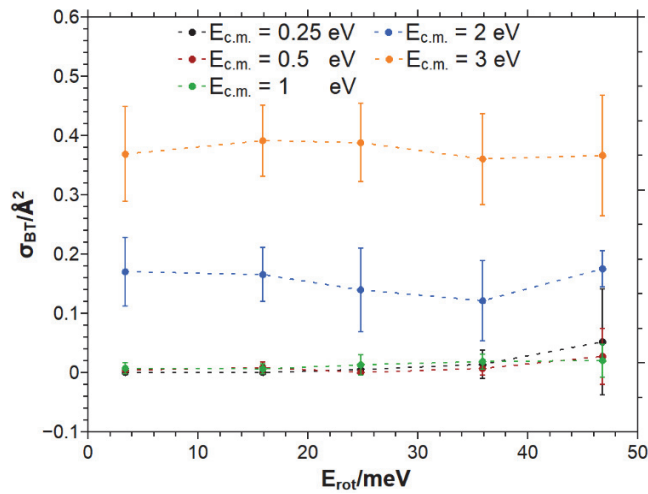


Figure S 5. Rotational energy dependence of the BT reaction for the investigated collision energies.

In Figure S 5 the dependency of the cross section  $\sigma_{\text{BT}}$  on the rotational energy of  $\text{HBr}^+$  is shown. For all collision energies investigated the cross section for BT reaction is basically independent of the  $\text{HBr}^+$  ion rotation within the error margins.

## 7. Supplementary Information – Potential energy surface of CH<sub>4</sub> + HBr<sup>+</sup> bimolecular reaction

Cartesian coordinates of the optimized geometries in the potential energy profile (Fig. 8) at CCSD(T)-F12/cc-pVDZ-PP-F12 level of theory

CH<sub>4</sub>

C	-0.0000014545	0.0000014806	-0.0000031665
H	0.2973342342	-0.1241088296	1.0387400214
H	0.8386157678	-0.2425025641	-0.6485790707
H	-0.3032825598	1.0304987606	-0.1695995035
H	-0.8326501100	-0.6639050102	-0.2205237143

HBr<sup>+</sup>

Br	0.0000000000	0.0000000000	-0.0180579196
H	0.0000000000	0.0000000000	1.4315336302

CH<sub>5</sub><sup>+</sup>

C	-0.0066008570	-0.0000005843	-0.0777386905
H	-0.5764302302	-0.0000006692	0.9699639969
H	-0.4045925439	-0.9376046137	-0.4546601162
H	1.0932729554	0.0000252959	-0.1884708912
H	-0.4046243963	0.9375938723	-0.4546523423
H	0.3710325607	-0.0000069221	1.0541834339

CH<sub>3</sub>

C	0.0000002990	-0.0000023925	0.0000015786
H	-0.0000011878	1.0414993985	-0.2755218802
H	-0.0000011879	-0.2821274686	1.0396913874
H	-0.0000011879	-0.7593434205	-0.7641883187

H<sub>2</sub>Br<sup>+</sup>

Br	0.0000000000	0.0246510713	0.0000000084
H	0.0000000000	-0.9771017399	1.0369007556
H	0.0000000000	-0.9771010936	-1.0369014246

CH<sub>4</sub><sup>+</sup>

C	-0.0000002369	-0.0000000005	0.0700889444
H	0.5460767204	0.0000017820	-0.9811770881
H	0.0000019139	-0.9617521835	0.5635738350
H	-0.5460757136	-0.0000017597	-0.9811773844
H	-0.0000000971	0.9617521667	0.5635738680

HBr

Br	0.0000000000	0.0000000000	-0.0176520490
H	0.0000000000	0.0000000000	1.3993584180

CH4Br<sup>+</sup>

Br	-0.0000000023	0.0191697825	-0.3179757925
C	0.0000000003	-0.0107681372	1.6690786362
H	-0.00000000853	-1.4036395493	-0.5092800640
H	-0.9135880041	-0.5169857551	1.9556424736
H	0.9135872355	-0.5169874970	1.9556418417
H	0.0000010301	1.0462539829	1.9160049776

i1

Br	0.0000062484	-0.0006943482	0.5697592178
C	0.0000657529	-0.0087846526	-2.7713158353
H	-0.9214393205	0.3790530024	-2.3161672920
H	0.9192099519	0.3852929684	-2.3168760172
H	-0.0009720837	0.1128901762	-0.9364099271
H	0.0037325884	-1.0956099664	-2.7842530308
H	-0.0018100090	0.3780992633	-3.7896415926

i2

Br	-0.0176905536	0.0000000186	-0.4976313155
C	0.0000687077	-0.0000007858	2.5442962874
H	1.4180475924	0.0000000245	-0.4764016563
H	0.5293036761	0.9208114299	2.7693625999
H	-1.0641891852	0.0012685991	2.7614133530
H	0.5271194414	-0.9220659853	2.7693584425
H	-0.0086894228	-0.0000061761	1.3069594902

i3

Br	0.0176865942	0.0000007645	0.4977178856
C	0.0004526499	-0.0000215618	-2.5447635634
H	-1.4179725927	-0.0000149478	0.4777173939
H	-1.0603283389	0.0349005803	-2.7736546216
H	0.5612171095	0.9035774783	-2.7640718061
H	0.5011307083	-0.9381143882	-2.7645659286
H	0.0084621911	-0.0001523930	-1.3074118330

i4

Br	0.0000035395	-0.0007817825	0.5775257308
C	0.0001383184	-0.0201284465	-2.7816957840
H	-0.0009928835	0.1501162439	-1.5058350877

H	0.9310398991	0.1155858052	-3.3242507183
H	-0.0053159317	-1.0259083720	-2.3359664417
H	-0.9268161647	0.1219584696	-3.3295214381
H	0.0001562310	0.9400816112	-2.1397696226

i6

Br	0.0198471207	0.0000024085	0.4446899609
C	0.0018811096	-0.0000105199	-2.4756988759
H	1.0804508323	0.0063432670	-2.5460690106
H	-0.5328145637	0.9289954661	-2.6169008846
H	-0.5218601189	-0.9353589828	-2.6160514979
H	-0.2356181994	-0.0000558037	1.8756554756
H	-1.3859457389	0.0000104810	0.1521431887

i7

Br	-0.0000010606	-0.0196677486	-0.4462360140
C	0.0000041678	-0.0029163996	2.4836301211
H	-0.9302655710	-0.5472431808	2.5640859258
H	0.9326335458	-0.5431675750	2.5642451669
H	-0.0023601170	1.0610912425	2.6770356858
H	0.0000341568	0.2380529597	-1.8764096892
H	-0.0000076013	1.3851716104	-0.1496834458

i9

Br	-0.0000095290	0.0402936607	0.2816405259
C	0.0000373568	-0.0788060141	-1.7006193063
H	-0.9132397558	-0.5972390845	-1.9654184533
H	0.9130039647	-0.5978294641	-1.9653345345
H	0.0003939369	0.9653134749	-1.9976065648
H	-0.0002551455	-1.3712290486	0.5404846292
H	0.0004072498	-0.6541953824	3.3261786973

ts-1-2

Br	0.0000043334	-0.0064969885	0.5367889121
C	-0.0033538428	-0.0184031026	-2.6257422463
H	0.0002858818	0.8379337517	-0.6540930771
H	0.1511029978	-0.2413767718	-3.6814015352
H	-1.0751036890	0.0415983930	-2.4381804120
H	0.5007728207	0.9351006107	-2.4271113778
H	0.4625641395	-0.8389116411	-2.0635657519

ts-1-4

Br	-0.0001292560	0.0000075462	-0.6880983861
C	-0.0112989885	0.0002829185	3.3016685465
H	1.0790046514	-0.0040194705	3.4848097933
H	-0.4296608885	0.9398813092	3.6501336748
H	0.4428051493	-0.0019887223	2.1973729089
H	-0.5112735080	-0.0026582366	2.2184586808
H	-0.4359856042	-0.9351844709	3.6539717835

ts-2-3

Br	-0.0000020780	-0.0176794617	-0.4977322526
C	-0.0000660829	-0.0004506106	2.5447593207
H	0.0023429395	-0.0093194250	1.3076767853
H	0.0000746034	1.4179340877	-0.4770118344
H	-0.0069655777	1.0609041767	2.7733817995
H	0.9240665633	-0.5257597390	2.7661962078
H	-0.9185663244	-0.5368579029	2.7629333304

ts-2a

Br	0.0000009288	-0.0172142353	0.4614224488
C	0.0000054251	-0.0039376370	-2.3187787046
H	-0.0000813245	1.4192722641	0.3678790219
H	-0.9515366648	0.0308882056	-1.7576742241
H	0.0013601286	-0.9573785638	-2.8471931377
H	0.9514984935	0.0336636062	-1.7578007131
H	-0.0013789071	0.8851278081	-2.9528152990

ts-2b

Br	-0.0188582507	0.0000000315	0.5579872774
C	0.0045301971	0.0000000604	-2.8992747188
H	1.3842032799	-0.0000012962	0.8078709128
H	0.0435996766	0.5411861355	-1.8411457111
H	-0.9687355451	0.0000019896	-3.3684534361
H	0.9383353927	0.0000004546	-3.4424477126
H	0.0435931552	-0.5411905041	-1.8411493372

ts-2-6

Br	-0.0000025273	-0.0223045015	0.4883093252
C	-0.0000415067	-0.0030082147	-2.6654661415
H	0.0440270533	-1.0819966036	-2.6124216428
H	0.9099785129	0.5455105436	-2.8637548113
H	-0.9532028374	0.4706696647	-2.8532170170
H	0.0000096967	0.7203046931	1.7282848123
H	-0.0001174666	1.1495382842	-0.3466803904

ts-6-7

Br	0.0000135547	-0.0000901967	-0.4820470144
C	0.0000028994	-0.0001090210	2.7418252943
H	-0.0003132602	-1.0247191343	-1.5001822929
H	-0.0003048201	1.0284324862	-1.4962190677
H	-0.0426772389	1.0750096754	2.8385596270
H	-0.9098602462	-0.5718982635	2.8494042658
H	0.9520464717	-0.4983753214	2.8498596021

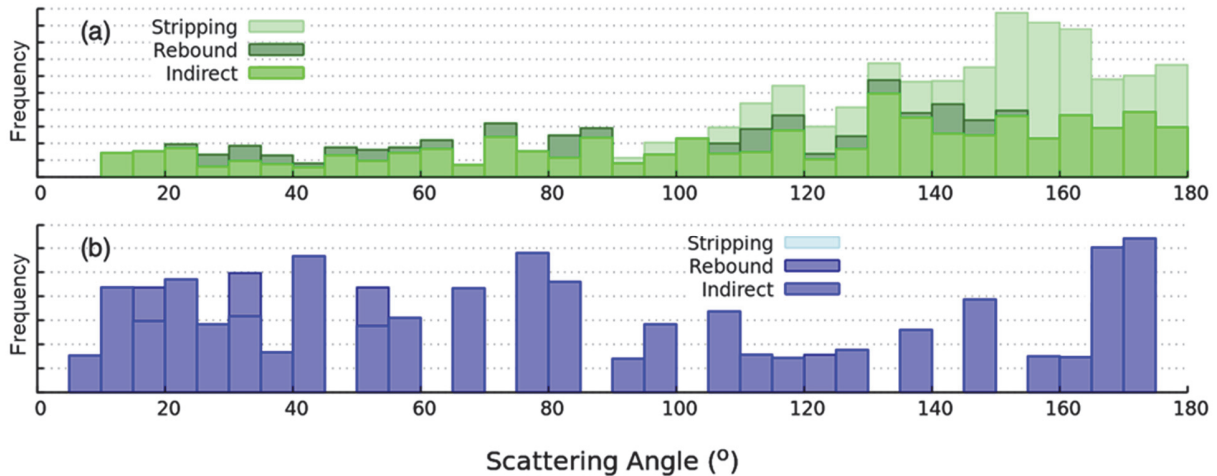
ts-3-7

Br	0.0223170015	0.0000338364	0.4877972324
C	0.0037674800	-0.0001241380	-2.6624987521
H	-0.7196521037	-0.0027983859	1.7281599692
H	-1.0430375124	0.0118522341	-2.9344492282
H	0.5594414559	0.9262790896	-2.6933479288
H	0.5389213852	-0.9384224096	-2.6958173840
H	-1.1497384402	0.0018863823	-0.3470991013

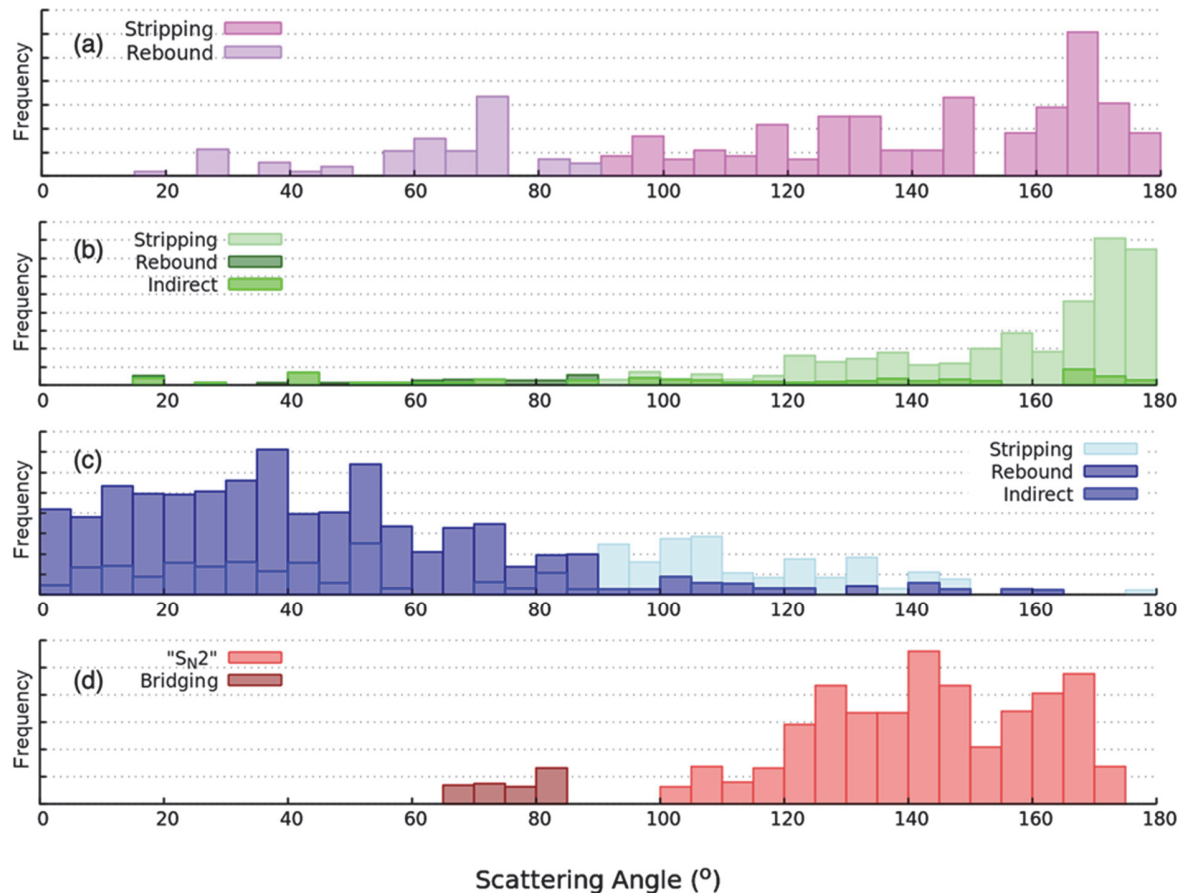
ts-6-9

Br	0.0000135547	-0.0000901967	-0.4820470144
C	0.0000028994	-0.0001090210	2.7418252943
H	-0.0003132602	-1.0247191343	-1.5001822929
H	-0.0003048201	1.0284324862	-1.4962190677
H	-0.0426772389	1.0750096754	2.8385596270
H	-0.9098602462	-0.5718982635	2.8494042658
H	0.9520464717	-0.4983753214	2.8498596021

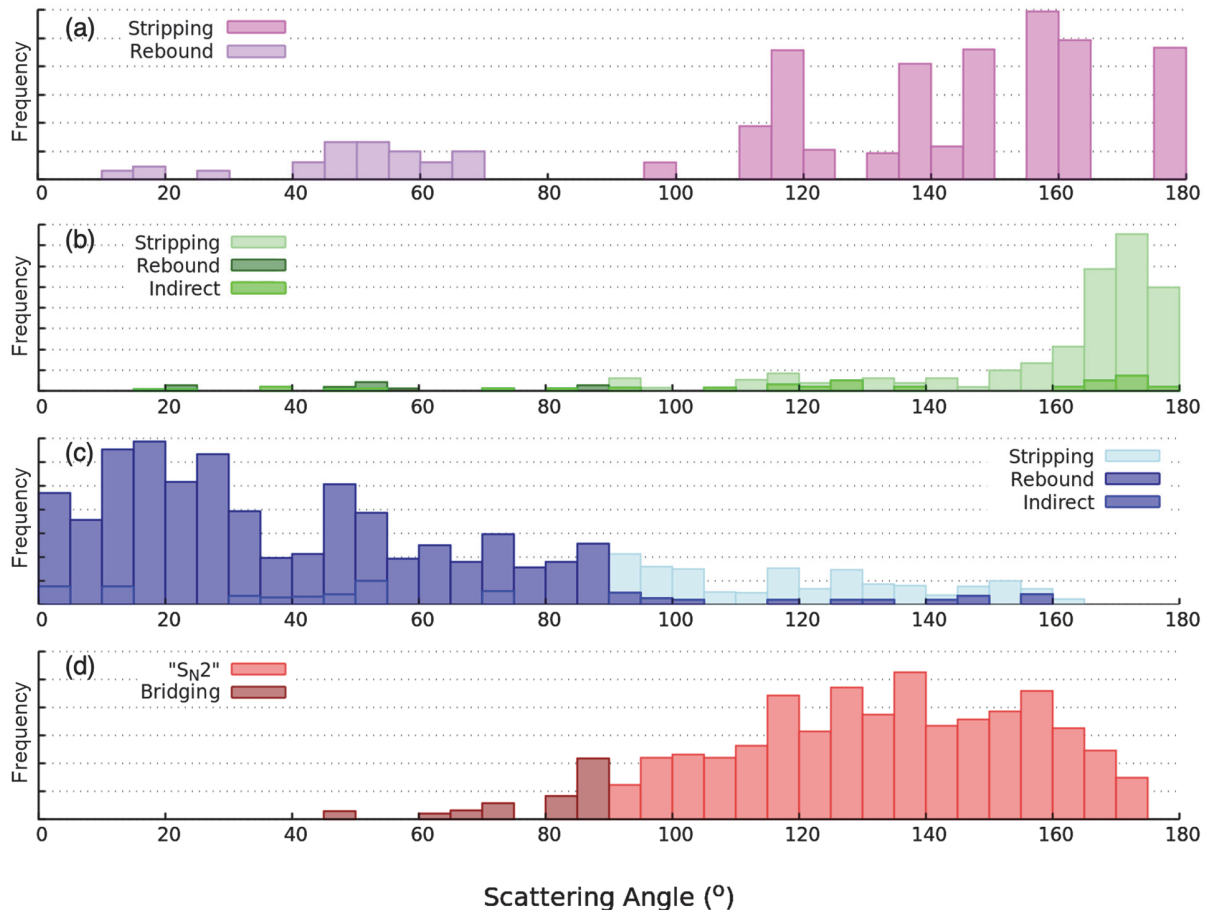
## 8. Scattering angle distributions for collision energies (0.5 eV, 2.0 eV and 3.0 eV) respectively



S7: Scattering angle distribution per mechanism for PT (a) and HA (b) product channels at 0.5 eV collision energy



S6: Scattering angle distribution per mechanism for CT (a), PT (b), HA (c) and BT (d) product channels at 2.0 eV collision energy.



S8: Scattering angle distribution per mechanism for CT (a), PT (b), HA (c) and BT (d) product channels at 3.0 eV collision energy